Interaction energies for blends based on glycidyl methacrylate copolymers

P. P. Gan and D. R. Paul*

Department of Chemical Engineering and Center for Polymer Research, University of Texas at Austin, Austin, TX 78712, USA

(Received 27 September 1993; revised 10 December 1993)

The phase behaviour of blends of glycidyl methacrylate/methyl methacrylate (GMA/MMA) copolymers with styrene/acrylonitrile (SAN) copolymers and of GMA/styrene copolymers with tetramethyl polycarbonate and poly(2,6-dimethyl-1,4-phenylene oxide) has been determined and analysed using two theoretical approaches. Binary interaction densities for repeat-unit pairs were evaluated from the lower critical solution temperature type phase behaviour using the lattice-fluid theory of Sanchez and Lacombe and from copolymer composition miscibility boundaries using the Flory–Huggins theory. For the GMA/MMA–SAN system the interaction energies obtained by the two approaches agree quite well with each other and with independent information obtained by the critical molecular-weight method.

(Keywords: copolymer blends; glycidyl methacrylate; interaction energies)

INTRODUCTION

Immiscible polymer blends often have poor mechanical properties relative to their components because of the unfavourable interaction between molecular segments at the interface between the phases, viz. a large interfacial tension, which leads to poor control of morphology during melt mixing, and poor interfacial adhesion or stress transfer in the solid state. An effective way to gain control of the morphology and to strengthen the interfacial zone is to form block or graft copolymers *in situ* during blend preparation via interfacial reaction of added functionalized polymeric components[1–7]. For example, Triacca *et al.* compatibilized blends of nylon-6 with acrylonitrile– butadiene–styrene (ABS) materials by adding styrene/ maleic anhydride (SMA) copolymers into ABS[8]. The SMA copolymer is miscible with the styrene/acrylonitrile (SAN) copolymer phase of ABS and also contains functional groups that can react with the nylon-6 to form *in situ* graft copolymers at the polymer–polymer interface. Certain styrene/acrylic acid (SAA) copolymers and SMA copolymers are miscible with the poly(methyl methacrylate) (PMMA) grafted chains of core–shell impact modifiers and can chemically react with the nylon-6[9,10]. These materials have been shown to be effective additives for dispersing such core–shell impact modifiers in nylon-6, leading to tough blends. Thus, polymeric additives that exhibit miscibility with one phase and chemical reactivity with the other have considerable utility for compatibilizing multiphase blends. There is a need for developing such materials where the reactive group is neither an acid nor an anhydride. The epoxide functionality in monomers like glycidyl methacrylate (GMA) is a promising candidate, as shown by recent studies[11,12].

To develop systematically the concept of using GMA as a functional monomer in reactive processing, it is first necessary to examine the phase behaviour of blends with copolymers containing GMA monomer. In this paper, the phase behaviour of blends containing copolymers of GMA with either methyl methacrylate (MMA) or styrene (S) will be examined. The GMA/MMA copolymers were blended with SAN copolymers to map the regions of copolymer composition where miscibility exists. The GMA/S copolymers were blended with tetramethyl polycarbonate (TMPC) and with poly(2,6-dimethyl-1,4-phenylene oxide) (PPO). Interaction energies for these systems were evaluated where possible from the copolymer–copolymer miscibility maps using the Flory–Huggins theory or from the observed phase-separation temperatures using the lattice-fluid theory of Sanchez and Lacombe[13–16]. The interaction energies obtained expand the matrix of known binary interaction energies[17–25] that are needed for accurate design of miscible blends. In this case, the objective is to explore the design of functional polymers for use in reactive processing.

EXPERIMENTAL

Tables 1 and *2* show the chemical compositions, molecular weight and T_g information for the various polymers used. The homopolymer of glycidyl methacrylate (PGMA) and its copolymers with styrene and MMA were synthesized via free-radical polymerization using 0.5% by weight of azobisisobutyronitrile (AIBN) based on momoner. The inhibitor was removed from commercial MMA and styrene monomers by extraction with an aqueous 10% sodium hydroxide solution, while the GMA was purified using vacuum distillation. Vacuum distillation of the GMA monomer is necessary to avoid any crosslinking of the polymer during the synthesis. Glass vials (volume 30 ml)

*To whom correspondence should be addressed

0032-3861/94/16/3513–12

Table 1 Glycidyl methacrylate-based copolymers synthesized for this study

Abbreviation	Copolymer composition (wt% GMA)	T_g (°C)	$\bar{M}_n$ (kg mol^{-1})	$\bar{M}_w$ (kg mol^{-1})	$\bar{M}_w/\bar{M}_n$
GMA/MMA5	4.6	107	162	303	1.88
GMA/MMA8	8.0	106	191	321	1.68
GMA/MMA14	14.0	102	208	348	1.67
GMA/MMA23	23.3	98	232	414	1.79
GMA/MMA29	28.6	94	242	418	1.73
GMA/MMA36	35.7	90	248	479	1.93
GMA/MMA46	46.1	87	243	473	1.95
GMA/MMA55	55.0	80	233	471	2.02
GMA/MMA60	60.1	73	251	472	1.88
GMA/MMA75	75.3	67	181	349	1.92
GMA/S2	1.6	102	130	212	1.63
GMA/S7	6.8	101	126	208	1.64
GMA/S14	14.0	99	130	205	1.58
GMA/S19	18.6	97	134	258	1.93
GMS/S26	25.6	93	139	239	1.72
GMA/S28	28.2	93	158	287	1.82
GMA/S33	33.3	87	179	344	1.92
GMA/S37	37.1	86	173	353	2.04
GMA/S43	43.5	83	195	407	2.08
GMA/S50	50.2	83	239	449	1.88
GMA/S66	66.2	79	319	601	1.88
PGMA	100.0	63	183	393	2.15

were filled with 20 ml of the monomer and initiator mixture and sealed under nitrogen atmosphere. The sealed vials were held in a thermostated bath at 60°C until a yield of approximately 10% of polymer was obtained. For PGMA, the polymer solution was then poured into dioxane and the polymer was precipitated with methanol. In the case of GMA/MMA and GMA/S copolymers, the solvents used in the purification procedure were benzene and chloroform, respectively. The polymer solutions containing the copolymers were then precipitated using methanol. The precipitate was isolated and dried in a vacuum oven.

The GMA content of the copolymer was estimated using a hydrochloric acid/dioxane titration method, which involves epoxide ring opening[26]. A copolymer sample (1% by weight) was added to 25 ml of the hydrochlorination reagent (prepared by addition of 1.6 ml of concentrated hydrochloric acid to 100 ml of purified dioxane). After 15 min of stirring at room temperature, neutral ethanol (25 ml, containing cresol red indicator) was added and the mixture was titrated with 0.1 N methanolic sodium hydroxide solution to the first violet colour of the end-point[27,28]. The GMA content of GMA/S copolymers obtained using this titration method were consistent with the results obtained from elemental analysis (Huffman Laboratories Inc.). Molecular-weight information for GMA/MMA copolymers and GMA/S copolymers was estimated by g.p.c. in tetrahydrofuran (THF), where PMMA and polystyrene were used as standards, respectively.

Glass transition temperatures were determined using a Perkin–Elmer DSC-7 at a heating rate of 20°C min^{-1}, using the onset method. *Figures 1* and *2* show the composition dependence of T_g for GMA/MMA and GMA/S copolymers. Note that the T_g found for PMMA is slightly lower than expected based on extrapolation of the copolymer data because the PMMA used is a

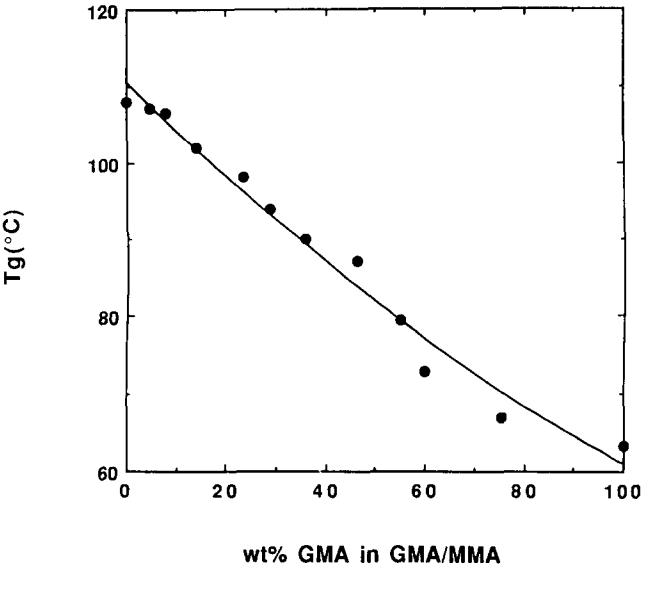

Figure 1 Glass transition temperature for GMA/MMA copolymers by d.s.c. (onset method) at 20°C min^{-1}

commercial material that contains a small amount of a comonomer, probably ethyl acrylate, to prevent unzipping. Blends of GMA/MMA copolymers with SAN copolymers were prepared by solution casting from THF, and cloud points were determined visually by heating on a hot stage (Mettler FP82 HT equipped with a Mettler FP80 HT temperature controller) at various constant temperatures for certain time periods[23,24]. Note that the T_g for some blends of GMA/MMA copolymers with SAN copolymers are too close to be resolved by d.s.c. Blends of GMA/S copolymers with TMPC and PPO were solution cast from THF and chloroform, respectively. Phase-separation

Table 2 Other polymers used in this study

Polymer	Molecular weight (kg mol^{-1})	AN (wt%)	Source
SAN	$\bar{M}_n$=93.5 $\bar{M}_w$=204	2.7	Asahi Chemical
SAN3.5	$\bar{M}_n$=93.0 $\bar{M}_w$=211	3.5	Asahi Chemical
SAN5.7	$\bar{M}_w$=270	5.7	Asahi Chemical
SAN6.3	$\bar{M}_n$=121 $\bar{M}_w$=343	6.3	Dow Chemical Co.
SAN9.5	$\bar{M}_n$=94.7 $\bar{M}_w$=195.6	9.5	Asahi Chemical
SAN11.5	-		Asahi Chemical
SAN13.5	$\bar{M}_n$=56.3 $\bar{M}_w$=149	13.5	Asahi Chemical
SAN14.7	$\bar{M}_n$=83.0 $\bar{M}_w$=182	14.7	Asahi Chemical
SAN15.5	$\bar{M}_w$=197	15.5	Asahi Chemical
SAN19.5	$\bar{M}_n$=84.3 $\bar{M}_w$=178.7	19.5	Asahi Chemical
SAN20.5	$\bar{M}_w$=193.8	20.5	Dow Chemical Co.
SAN24	$\bar{M}_n$=66.7 $\bar{M}_w$=113	24.0	Monsanto
SAN25	$\bar{M}_n$=77.0 $\bar{M}_w$=152	25	Dow Chemical Co.
SAN28	-	28	Asahi Chemical
SAN32.3	$\bar{M}_n$=50.7 $\bar{M}_w$=75.4	32.3	Monsanto
SAN33	$\bar{M}_n$=68.0 $\bar{M}_w$=146	33	Monsanto
SAN40	$\bar{M}_n$=61.0 $\bar{M}_w$=122	40	Asahi
SAN58.8	$\bar{M}_n$=32.1 $\bar{M}_w$=50.2	58.8	Monsanto
SAN62.6	$\bar{M}_n$=37.4 $\bar{M}_w$=55.9	62.6	Monsanto
SAN69	-	69.2	Monsanto
PMMA	$\bar{M}_n$=52.9 $\bar{M}_w$=105.4	108	Rohm and Haas, V(811)100
PS	$\bar{M}_n$=100 $\bar{M}_w$=330	104	Cosden Oil and Chem. Co., Cosden 550
TMPC	$\bar{M}_w$=33.0	-	Bayer AG
PPO	$\bar{M}_n$=29.4 $\bar{M}_w$=39.0	-	General Electric Co.

temperatures for these copolymer/homopolymer blends were determined using a d.s.c. technique[22–24]. Extreme care was taken to ensure that the phase-separation temperatures reported here reflect an equilibrium phase diagram of the lower critical solution temperature (*LCST*) type[22].

The density of PGMA was determined at 30°C by a density gradient column using calcium nitrate solutions. Changes in specific volume as a function of temperature and pressure were measured using a Gnomix PVT apparatus. The characteristic parameters of the Sanchez–Lacombe theory were computed for GMA/MMA and GMA/S copolymers from homopolymer parameters for PGMA, PMMA and PS using the mixing rules described earlier[22].

THEORY

In the following sections, the phase behaviour of the various blends will be analysed to obtain interaction energies using a binary interaction model for copolymers combined with either the Flory–Huggins or the Sanchez–Lacombe theories. For the former, the free energy of mixing per unit volume is given by:

$$\Delta g_{mix} = RT\left(\sum_{i=1}^{2} \frac{\phi_i \ln \phi_i}{\tilde{V}_i}\right) + B\phi_1\phi_2 \qquad (1)$$

where R is the universal gas constant, T is the absolute temperature and ϕ_i and $\tilde{V}_i$ are the volume fraction and molar volume of component i, respectively. If the interaction energy in equation (1) does not depend on composition, differentiation of the equation leads to the familiar spinodal equation:

$$\frac{d^2(\Delta g)}{d\phi_1^2} = RT\left(\frac{1}{\phi_A \tilde{V}_A} + \frac{1}{\phi_B \tilde{V}_B}\right) - 2B_{sc} = 0 \qquad (2)$$

where B_{sc} is the interaction parameter at the spinodal condition. This form is often used even though the interaction energy does depend on composition. Therefore, equation (2) leads to a new interaction energy, i.e.:

$$B_{sc} = -\frac{1}{2}\frac{d^2(\Delta g_{nc})}{d\phi_1^2} \qquad (3)$$

where Δg_{nc} is the non-combinatorial free energy. The subscript sc will be omitted and B will be understood to mean B_{sc} unless otherwise stated.

According to the binary interaction model for a blend of copolymer A composed of units 1 and 2 with another copolymer B composed of units 3 and 4, the net interaction energy B is given by:

$$B = B_{13}\phi_1'\phi_3'' + B_{14}\phi_1'\phi_4'' + B_{23}\phi_2'\phi_3'' + B_{24}\phi_2'\phi_4'' - B_{12}\phi_1'\phi_2'' - B_{34}\phi_3'\phi_4'' \qquad (4)$$

where ϕ_k' and ϕ_k'' denote the volume fractions of k units in copolymers A and B. The critical condition for miscibility obtained from the Flory–Huggins theory, when the interaction energy is not composition-dependent,

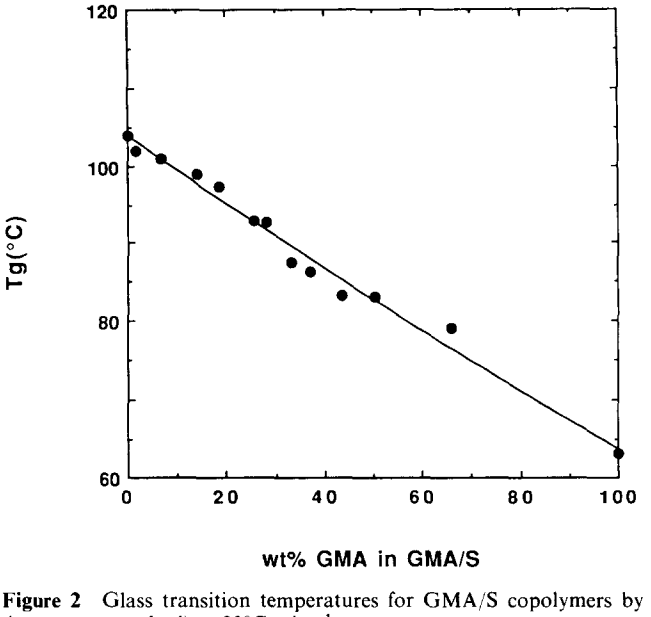

Figure 2 Glass transition temperatures for GMA/S copolymers by d.s.c. (onset method) at 20°C min^{-1}

is:

$$B_{crit} \leqslant \frac{RT}{2}\left(\frac{1}{\tilde{V}_A^{1/2}}+\frac{1}{\tilde{V}_B^{1/2}}\right)^2 \quad (5)$$

When the molecular weights or molar volumes of the components (weight-average values) are fixed for a copolymer–copolymer system, equation (4) predicts an elliptical, parabolic or hyperbolic isothermal map of copolymer compositions dividing miscible from immiscible mixtures. There are altogether six unknown B_{ij} values required to describe such a system, and some information about them can be deduced from an experimental miscibility map. However, the set of B_{ij} values used to map a miscibility region may be scaled by an arbitrary non-zero real number and still give the same miscibility region. Therefore, the most information that can be extracted from the miscibility region is only the relative ratios of B_{ij} values, in the case of high-molecular-weight systems where the combinatorial entropy is small. In order to obtain absolute B_{ij} values, at least one has to be obtained from an independent experiment.

An alternative, at least in principle, is to make use of more phase diagram information than simply the miscibility maps, e.g. phase-separation temperatures when they exist. However, the Flory–Huggins theory is frequently not able to make use of such data, since this simple theory does not predict *LCST* behaviour. For this reason it is useful to employ an equation-of-state theory that *can* predict *LCST* behaviour stemming from the compressible nature of polymers. Here, the lattice-fluid theory of Sanchez and Lacombe is employed to describe such effects. Detailed descriptions of this theory and its application to polymer blends have been given extensively in previous papers[13–16,18–25]. The lattice-fluid equation of state has the following simple closed form:

$$\tilde{\rho}^2+\tilde{P}+\tilde{T}[\ln(1-\tilde{\rho})+(1-1/r)\tilde{\rho}]=0 \quad (6)$$

where the reduced properties are defined as $\tilde{P}=P/P^*$, $\tilde{T}=T/T^*$ and $\tilde{\rho}=v^*/v$, and r is a chain length given by:

$$r=MP^*/kT^*\rho^*=M/\rho^*v^* \quad (7)$$

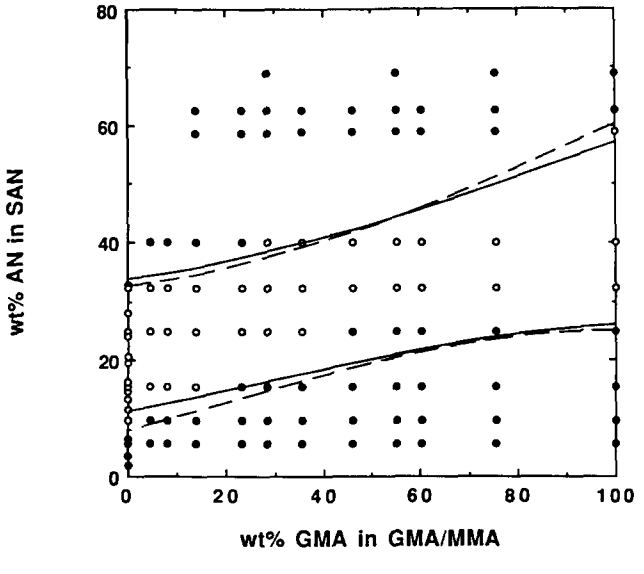

Figure 3 Miscibility map at 100°C for 50/50 wt% blends of GMA/MMA copolymers with SAN copolymers at 100°C: (○) miscible; (●) immiscible. The full curves were calculated from the B_{ij} set obtained from *LCST* data, while the broken curves were calculated from the B_{ij} set obtained from the best fit of the miscibility map (see *Table 5* for values)

Table 3 Phase-separation temperatures for 50/50 wt% blends of GMA/MMA and SAN copolymers[a]

AN (wt%) in SAN	GMA (wt%) in GMA/MMA	Phase-separation temperature (°C)
32.3	0	169
	4.6	174
	8.0	184
	14.0	187
	23.3	246
	28.6	271
40.0	28.6	181
	35.7	187
	46.1	222

[a] Note: all the other miscible blends did not phase-separate prior to thermal degradation

P^*, T^*, ρ^*, v^* and M are the characteristic pressure, temperature, density, hard-core volume per mer and weight-average molecular weight, respectively. Mixing rules for the characteristic parameters used here are the ones given by Sanchez and Lacombe[15].

In this theory, a bare interaction energy density, ΔP^*, replaces the B in the Flory–Huggins theory. For a copolymer–copolymer system, the same binary interaction energy framework can be used, i.e.:

$$\Delta P^* = \Delta P^*_{13}\phi'_1\phi''_3+\Delta P^*_{14}\phi'_1\phi''_4+\Delta P^*_{23}\phi'_2\phi''_3+\Delta P^*_{24}\phi'_2\phi''_4 -\Delta P^*_{12}\phi'_1\phi''_2-\Delta P^*_{34}\phi'_3\phi''_4 \quad (8)$$

where ΔP^*_{ij} are the binary pair interaction energies and ϕ'_k refer to hard-core volume fractions. The spinodal condition for a binary mixture is given by:

$$\frac{d^2G}{d\phi_1^2}=\frac{1}{2}\left(\frac{1}{r_1\phi_1}+\frac{1}{r_2\phi_2}\right)-\tilde{\rho}\left(\frac{\Delta P^*v^*}{kT}+\frac{\psi^2\tilde{T}P^*\beta}{2}\right)=0 \quad (9)$$

where ψ is a dimensionless function described elsewhere[15] and β is the isothermal compressibility factor.

BLENDS OF GMA/MMA WITH SAN COPOLYMERS

Figure 3 shows the miscibility map for 50/50 wt% blends of GMA/MMA copolymers with SAN copolymers. Miscible and immiscible blends are indicated by the open and full circles, respectively. As expected, blend films prepared by solution casting were transparent for miscible blends and cloudy for immiscible blends. The miscibility region includes the well known window of miscibility for PMMA with SAN copolymers that extends from 9.5 to 32.3 wt% AN[29–37] and shifts to higher AN levels as GMA is added to the MMA-based copolymers. Most of the miscible blends did not phase-separate prior to thermal degradation. However, for a few copolymer–copolymer compositions, phase-separation temperatures were observed, and these are indicated in *Table 3*. The blend phase-separation temperature increases as the GMA content in the GMA/MMA copolymer increases when the AN content of the SAN copolymer is held fixed. PGMA is miscible with SAN containing 32.3 to 58.8 wt% AN and the phase-separation temperatures of these blends are all above the thermal degradation limit of 300°C.

The observed phase-separation temperatures may be used to calculate the interaction energy densities using

the Sanchez–Lacombe theory. The analysis employed assumes that the experimental phase-separation temperatures correspond to the spinodal curve and that ΔP^* does not depend on temperature[38]. The former is certainly a good approximation near the critical composition, and the results that follow were extracted from information in this region. The latter assumption is believed to be reasonable for systems that do not involve strong specific interactions. The characteristic parameters required by the equation-of-state theory (T^*, P^* and ρ^*) have been determined previously for SAN copolymers from *PVT* data[22–25]. In the case of GMA/MMA copolymers, the characteristic parameters were calculated from values for PGMA and PMMA homopolymers using the mixing rules[22–25]. *PVT* data for PMMA have been determined previously[23]; however, this information for PGMA had to be determined and is reported here. *Figure 4* shows the specific volume as a function of temperature and pressure for PGMA. *Table 4* lists the entire *PVT* data obtained for PGMA from isothermal experiments. Using a non-linear least-squares fitting, the characteristic parameters for PGMA are $T^* = 727$ K, $P^* = 5861$ bar and $\rho^* = 1.3143$ g cm^{-3} for the temperature range of 150–200°C and pressure range of 0–500 bar. The PGMA data above T_g were also fitted to the Tait equation[39–41]:

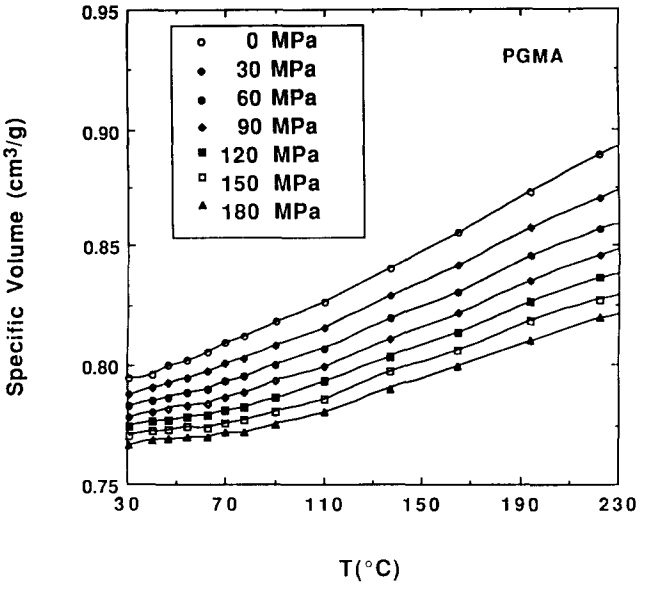

Figure 4 Specific volume of PGMA as a function of temperature and pressure

$$V(p, T) = V(0, T)\{1 - 0.0894 \ln[1 + p/C(T)]\} \quad (10)$$

where $V(p, T)$ is the specific volume (cm^3 g^{-1}) at pressure p (bar) and temperature T(°C). The temperature dependence of the specific volume at zero pressure, $V(0, T)$, and the parameter $C(T)$ are represented by the forms:

$$C(T) = C_0 \exp(-b_1 T) \quad (11)$$

$$V(0, T) = a_0 + a_1 T + a_2 T^2 \quad (12)$$

The Tait parameters for PGMA in the liquid state are as follows:

$$a_0 = 0.7729 \text{ cm}^3 \text{ g}^{-1}$$
$$a_1 = 4.48 \times 10^{-4} \text{ cm}^3 \text{ g}^{-1} \text{ °C}^{-1}$$
$$a_2 = 3.41 \times 10^{-7} \text{ cm}^3 \text{ g}^{-1} \text{ °C}^{-2}$$
$$C_0 = 3288 \text{ bar}$$
$$b_1 = 4.66 \times 10^{-3} \text{ °C}^{-1}$$

Table 4 Specific volume (cm^3 g^{-1}) of PGMA as a function of temperature and pressure in the liquid state

P (MPa)	77.7°C	90.2°C	110.4°C	137.1°C	164.6°C	194.2°C	222.1°C
0	0.8119	0.8179	0.8265	0.8406	0.8554	0.8732	0.8889
10	0.8088	0.8147	0.8228	0.8365	0.8506	0.8677	0.8823
20	0.8056	0.8114	0.8190	0.8325	0.8455	0.8619	0.8758
30	0.8031	0.8084	0.8158	0.8287	0.8414	0.8575	0.8704
40	0.8005	0.8057	0.8128	0.8254	0.8377	0.8531	0.8654
50	0.7977	0.8030	0.8098	0.8224	0.8340	0.8490	0.8610
60	–	0.8004	0.8072	0.8194	0.8302	0.8454	0.8567
70	–	0.7981	0.8045	0.8162	0.8270	0.8416	0.8526
80	–	0.7955	0.8023	0.8134	0.8238	0.8383	0.8490
90	–	0.7935	0.7994	0.8108	0.8212	0.8349	0.8456
100	–	–	0.7973	0.8085	0.8183	0.8320	0.8420
110	–	–	0.7952	0.8060	0.8158	0.8290	0.8387
120	–	–	0.7932	0.8036	0.8134	0.8261	0.8360
130	–	–	0.7907	0.8014	0.8105	0.8234	0.8326
140	–	–	0.7890	0.7992	0.8084	0.8210	0.8300
150	–	–	–	0.7974	0.8060	0.8182	0.8279
160	–	–	–	0.7950	0.8038	0.8154	0.8241
170	–	–	–	0.7930	0.8015	0.8133	0.8218
180	–	–	–	0.7905	0.7993	0.8100	0.8193
190	–	–	–	0.7882	0.7962	0.8082	0.8163
200	–	–	–	0.7864	0.7940	0.8063	0.8134

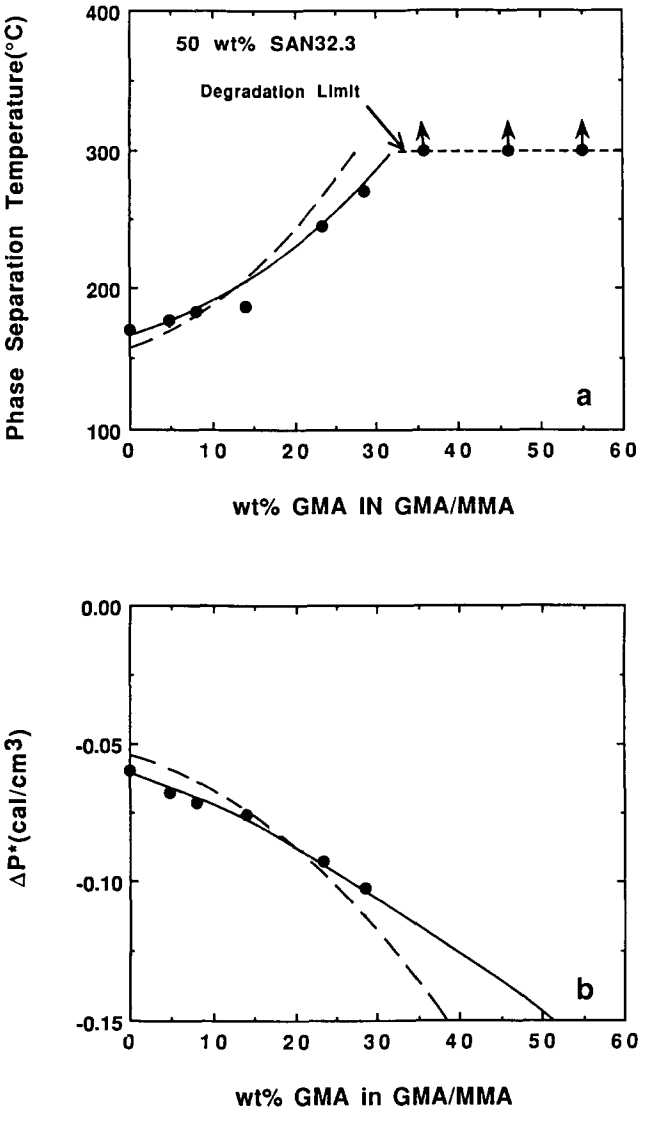

Figure 5 (a) Phase-separation temperatures and (b) bare interaction parameters for 50/50 blends of GMA/MMA copolymers with SAN32.3. The arrows indicate phase-separation temperatures above the thermal degradation limit. The points in part (b) were calculated from the experimental phase diagram using the lattice-fluid theory. The full and broken curves in (a) and (b) were calculated from the ΔP^*_{ij} set obtained from *LCST* data and the miscibility map, respectively (see *Table 5* for values)

Figure 5a shows the phase-separation temperatures for SAN32.3 with GMA/MMA copolymers. The full circles with arrows represent miscible blends that phase-separate at temperatures above the thermal degradation limit. Full circles in *Figure 5b* correspond to ΔP^* calculated from phase-separation temperatures given in *Figure 5a* using the Sanchez–Lacombe theory. If ΔP^* can be determined in this way over a broad enough range of compositions of the two copolymers, then, in principle, a non-linear regression of this information to equation (8) can be used to extract the various ΔP^*_{ij} values involved. However, when ΔP^* is only known over a limited range of copolymer compositions, as in the present case, then fewer parameters can be extracted from such an analysis. Previous work has led to relatively reliable estimates for all the ΔP^*_{ij} not involving GMA as one of the components. Thus, we set $\Delta P^*_{S/MMA} = 0.23$, $\Delta P^*_{MMA/AN} = 4.44$ and $\Delta P^*_{S/AN} = 7.37$ cal cm^{-3} from previous work[22]. The remaining interaction parameters involving GMA listed in *Table 5* were extracted by a non-linear regression of all the ΔP^* computed from the observed phase-separation temperatures listed in *Table 3*. In subsequent discussions, this set is referred to as the one deduced from the *LCST* data. The full curves in *Figures 5a* and *5b* were calculated from this set of ΔP^*_{ij}. The estimated spinodal curve and experimental phase-separation temperatures coincide very well. *Figures 6* and *7* compare the experimental (circles) and predicted (full curves) phase-separation temperatures for 50/50 wt% GMA/MMA14 and GMA/MMA29 as the AN content in the SAN copolymers varies using the *LCST* ΔP^*_{ij} from *Table 5*. The arrows on the open circles indicate that the phase-separation temperatures for these blends lie below the drying temperature of 100°C, while arrows on full circles represent miscible blends whose phase-separation temperatures are above the decomposition limit. The experimental data points and the predictions match

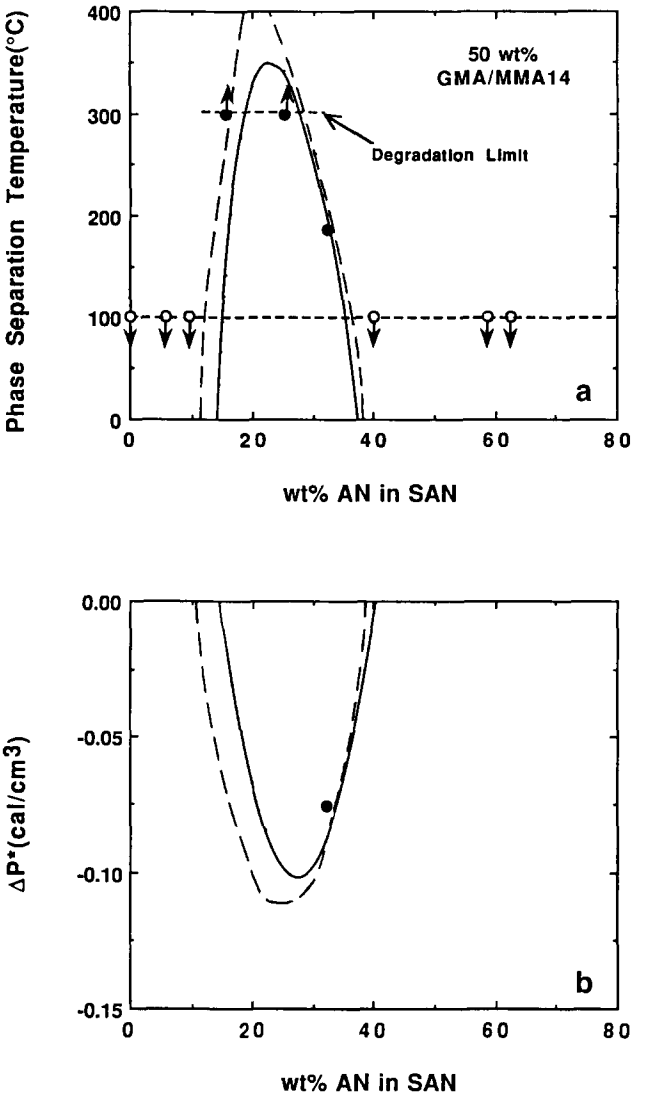

Figure 6 (a) Phase-separation temperatures and (b) bare interaction parameters for 50/50 blends of GMA/MMA14 with SAN copolymers. The horizontal broken line in (a) at 100°C represents the blend drying temperature. Arrows on the full and open points correspond to blends with phase-separation temperatures above the thermal degradation limit and below the drying temperature, respectively. The points in part (b) were calculated from the experimental phase diagram using the lattice-fluid theory. The full and broken curves were calculated from the ΔP^*_{ij} set obtained from the *LCST* data and miscibility map, respectively (see *Table 5* for values)

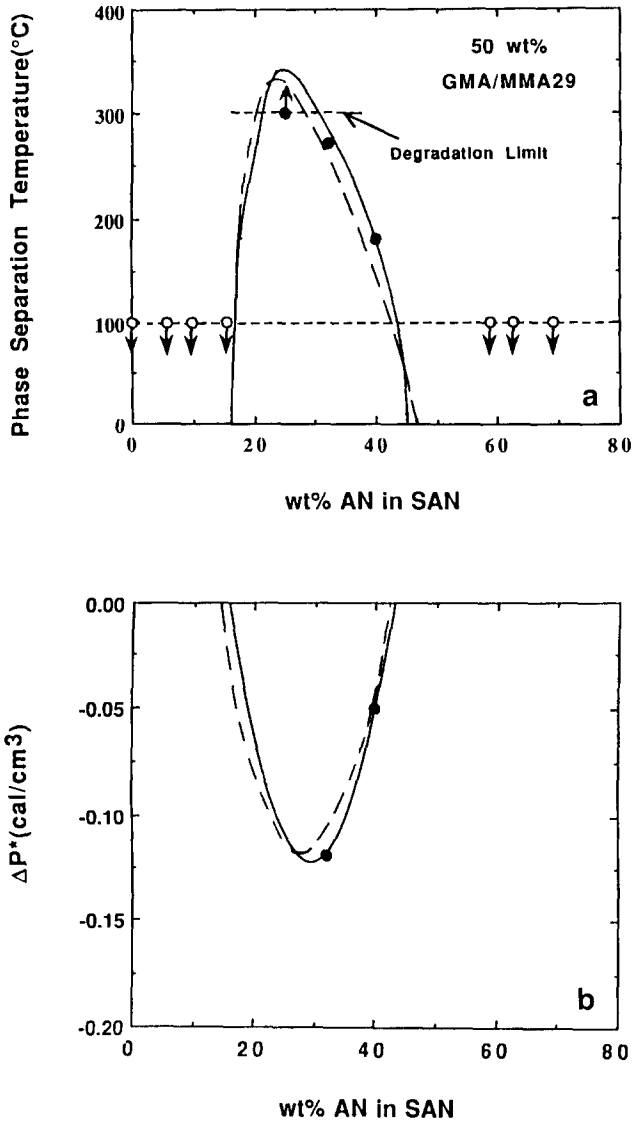

Figure 7 (a) Phase-separation temperatures and (b) bare interaction parameters for 50/50 blends of GMA/MMA29 with SAN blends copolymers. Lines, curves and points have same meaning as in *Figures 5* and *6*

relatively well. In addition, the region of copolymer compositions that form miscible and immiscible blends, represented by the full and open circles, respectively, are bounded by the spinodal curve quite well. A set of Flory–Huggins interaction energy densities, B_{ij}, can be calculated from these ΔP^*_{ij} from the following equation[22]:

$$B_{sc} = \tilde{\rho}\,\Delta P^* + \Bigg[P_2^* - P_1^* + (\phi_2 - \phi_1)\Delta P^* + \frac{RT}{\tilde{\rho}}\left(\frac{1}{r_1^0 v_1^*} - \frac{1}{r_2^0 v_2^*}\right) - RT\left(\frac{\ln(1-\tilde{\rho})}{\tilde{\rho}^2} + \frac{1}{\tilde{\rho}}\right)\left(\frac{1}{v_1^*} - \frac{1}{v_2^*}\right)\Bigg]^2 \Bigg/ \left[\frac{2RT}{v^*}\left(\frac{2\ln(1-\tilde{\rho})}{\tilde{\rho}^3} + \frac{1}{\tilde{\rho}^2(1-\tilde{\rho})} + \frac{(1-1/r)}{\tilde{\rho}^2}\right)\right] \quad (13)$$

The results obtained at the drying temperature of 100°C are shown in *Table 5*[22,24] under the *LCST* heading. The full curves shown in *Figure 3* were calculated from this set of B_{ij} values using equations (4) and (5). Note that the lines separate the miscible and immiscible blends relatively well.

A set of Flory–Huggins interaction energies B_{ij} can also be obtained by fitting equations (4) and (5) to the experimental composition map shown in *Figure 3*. The B_{ij} values extracted in this way are compared in *Table 5* to the set obtained from *LCST* data. Each point on the copolymer–copolymer phase map in *Figure 3* either does or does not satisfy the thermodynamic criterion given by equation (5). This may may be interpreted as an isothermal plane defined by the drying condition at 100°C. To avoid the trial-and-error fitting methods generally used[32,42–46], a computer program was developed to find the set of B_{ij} that best describes the experimental miscibility boundary by minimizing an objective function[47]. The objective function was defined as the sum of the squares of the orthogonal distances of the experimental data points (nearest to the miscibility boundary) to the theoretical boundary curve. Since at least one B_{ij} must be known independently, as explained earlier, the regression was performed with $B_{S/AN}$ set at 7.07 cal cm^{-3} (corresponds to $\Delta P^*_{S/AN} = 7.37$ cal cm^{-3} obtained in previous studies[22–24]). We chose to set $B_{S/AN}$ instead of $B_{S/MMA}$ as in past studies, since $B_{S/AN}$ is much larger in magnitude than $B_{S/MMA}$. Thus, small absolute errors in $B_{S/MMA}$ translate into large relative errors for all other B_{ij} values derived from such an analysis. The well known miscibility window for blends of PMMA with SAN copolymers is reproduced by $B_{S/MMA} = 0.16$ and $B_{MMA/AN} = 4.62$ cal cm^{-3} when $B_{S/AN} = 7.07$ cal cm^{-3}. The B_{ij} values involving GMA as one component were obtained by fitting the experimental data in *Figure 3* to equations (4) and (5) through minimization of the objective function mentioned. This set, listed in *Table 5* under the heading 'miscibility map', was used to calculate the broken curves shown in *Figure 3*. The B_{ij} values obtained from mapping the miscibility region were used to calculate the set of ΔP^*_{ij} values, via equation (13), shown in *Table 5* under the same heading. The phase-separation temperatures predicted using this latter set are shown by the broken curves in *Figures 5, 6* and *7*. Naturally, the interaction energies derived from phase-separation temperatures fit these data better than do the interaction energies deduced from mapping the copolymer miscibility boundaries. The converse is also true. However, the individual interaction energies determined by the two approaches agree with each other relatively well. The differences, expressed as percentages,

Table 5 Interaction energy densities (cal cm^{-3}) calculated for blends of GMA/MMA and SAN copolymers

	Obtained by fitting of			
	LCST data		Miscibility map	
Interaction pair	ΔP^*_{ij}	B_{ij}[a]	ΔP^*_{ij}[b]	B_{ij}[c]
S/MMA	0.23	0.23	0.16	0.16
MMA/AN	4.44	4.42	4.65	4.62
GMA/S	0.99	0.92	1.04	0.98
GMA/AN	2.37	2.50	2.09	2.25
GMA/MMA	0.17	0.15	0.12	0.11
S/AN	7.37	7.07	7.37	7.07

[a] Computed from ΔP^*_{ij} using equation (8) for 100°C
[b] Computed from B_{ij} using equation (8)
[c] Determined at 100°C

Table 6 Summary of results of blends of PGMA ($\bar{M}_w = 393\,000$ g mol^{-1}) with polymers of varying molecular weights

Polymer	Designation[a]	$\bar{M}_w$[b]	$\bar{M}_w/\bar{M}_n$[b]	T_g (°C)	End-group[c] (wt%)	No. of T_g	Film appearance
Poly(methyl methacrylate)	PMMA(1.21)	1210	1.16	31	11.5	1	Clear
Poly(methyl methacrylate)	PMMA(2.4)	2400	1.09	77	5.41	1	Clear
Poly(methyl methacrylate)	PMMA(4.25)	4250	1.07	99	3.00	1	Clear
Poly(methyl methacrylate)	PMMA(10.6)	10600	1.11	108	1.25	2	Cloudy
Poly(methyl methacrylate)	PMMA(20.3)	20300	1.11	125	0.65	2	Cloudy
Poly(α-methylstyrene)	PαMS(3.5)	3500	1.06	141	1.73	1	Clear
Poly(α-methylstyrene)	PαMS(6.7)	6700	1.06	160	0.90	2	Cloudy
Poly(α-methylstyrene)	PαMS(19.5)	19500	1.03	169	0.30	2	Cloudy
Polystyrene	PS(0.58)	580	1.18	−23	11.5	2	Cloudy

[a] The number in parentheses corresponds to the weight-average molecular weight in thousands
[b] Molecular-weight information from supplier (Polymer Laboratories Ltd)
[c] PMMA has a cumyl end-group, while PαMS and PS have n-butyl end-groups

for the small interaction energies for S/MMA and GMA/MMA are much larger (~39%) than for the larger interaction energies (~5–10%). Both sets of interaction energies fit the various data in an acceptable manner, so no preferences can be definitively expressed on this basis for one over the other.

Since there is no other information in the literature about interactions involving GMA units, it would be useful to attempt to get some independent assessment of the reliability of the estimates shown in *Table 5*. From the current experimental observations, PGMA is not miscible with either PMMA or PS when each component has a high molecular weight. These facts are correctly indicated by the positive interaction energy densities for these pairs. More refined estimates for the GMA interaction energies with PS and PMMA can be obtained by the critical molecular-weight method[18–21] since both PMMA and PS are available in monodisperse form over a wide range of molecular weights. *Table 6* shows the molecular-weight and miscibility information for blends of PGMA with PMMA and PS of varying molecular weight. Blends were prepared either by solution casting from THF onto a hot plate heated at 60°C or by precipitation from THF into methanol. Blends of PGMA ($\bar{M}_w = 393\,000$) were miscible with PMMA having $\bar{M}_w = 4250$ or a lower molecular weight. Miscible blends showed clear films and one T_g by d.s.c. but did not show any *UCST*- or *LCST*-type behaviour. PGMA is immiscible with PMMA at $\bar{M}_w = 10\,600$ and higher. Analysis of these observations using equation (5) reveals that $0.06 < B_{GMA/MMA} < 0.13$ cal cm^{-3}. Previous analyses using the critical molecular-weight method[18–21] indicate that corrections for end-group effects are sometimes necessary. PMMA has a cumyl end-group, which we will approximate as an α-methylstyrene (αMS) unit. Using the results in *Table 6* on the state of miscibility of blends of PGMA with PαMS of varying molecular weight shows that $B_{\alpha MS/GMA}$ must lie between 0.08 and 0.14 cal cm^{-3}. From the observations of Callaghan and Paul[19], values of $\Delta P^*_{\alpha MS/MMA} = -0.08$ and $B_{\alpha MS/MMA} = 0.07$ cal cm^{-3} at 100°C can be calculated. Using this information, end-group effects were taken into account, as described previously[18–21]. This leads to the following slightly revised range, $0.06 < B_{GMA/MMA} < 0.15$ cal cm^{-3}. The values of $B_{GMA/MMA}$ shown in *Table 5* fall within this range. Thus, we believe these estimates are quite realistic.

The interaction energy for GMA with styrene extracted from the *LCST* data or the miscibility map approach can also be verified using the critical molecular-weight method. Blends of PGMA were blended with the smallest molecular weight of PS(0.58) by solution casting from THF. This blend was cloudy and two T_g values were exhibited using d.s.c. From this observation, it can be concluded that $B_{GMAS/S} > 0.77$ cal cm^{-3} (ignoring end-group effects). To obtain more detailed information about $B_{GMA/S}$, lower molecular weights of PGMA could be synthesized and blended with the monodisperse PS series. This was not done; however, the lower limit for $B_{GMA/S}$ from the current critical molecular-weight experiments is consistent with the estimates shown in *Table 5*.

Table 5 lists two values for $B_{S/MMA}$ and, for reasons described below, we feel that $B_{S/MMA} = 0.23$ cal cm^{-3} is the more reliable one. The lower value of $B_{S/MMA} = 0.16$ cal cm^{-3} is closer to the value deduced by Fukuda *et al.*[48–50] from light scattering measurements on dilute ternary mixtures of PS and PMMA in a solvent. The latter has been used extensively in the past for the analysis of miscibility windows of blends of copolymer systems to obtain other interaction energies[29,37,51–55]. A recent reanalysis of data for blends of PMMA with SAN copolymers that made use of phase-separation temperatures as well as the SAN compositions at the edge of the miscibility window led to $B_{S/MMA} = 0.23$ cal cm^{-3} at 120°C[22]. In addition, a re-examination of data for blends of tetramethyl bisphenol A polycarbonate with SMMA copolymers[17] led to $\Delta P^*_{S/MMA} = 0.25$ cal cm^{-3}, which according to equation (13) corresponds to $B_{S/MMA} = 0.24$ cal cm^{-3} at 100°C. Callaghan *et al.*[19] found $B_{S/MMA} = 0.26$ cal cm^{-3} using the critical molecular-weight method. This value is about 20% higher than the value calculated from the χ parameter determined by Russell *et al.*[56] using small-angle neutron scattering from a symmetric, diblock copolymer, P(S-*b*-PMMA), where the PS block was deuterated. Recently, Russell *et al.*[57] re-examined this issue by deuterating both the PS and PMMA block. When both blocks are labelled, there appears to be an offsetting effect of the labelling, i.e. χ is lower. Using this lower value of χ leads to $B_{S/MMA} = 0.24$ cal cm^{-3} at 100°C, which is essentially identical to the value of 0.23 cal cm^{-3} recommended here.

The miscibility maps for binary blends of SAN

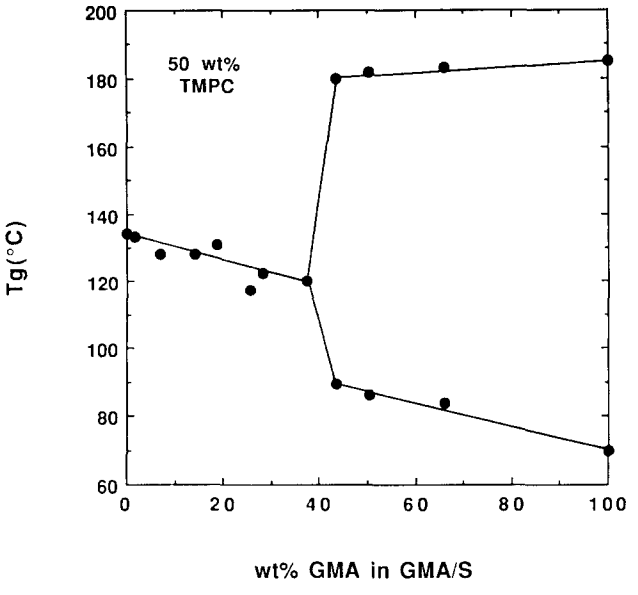

Figure 8 Glass transition temperatures for 50/50 wt% blends of TMPC with GMA/S copolymers by d.s.c. (onset method) at 20°C min^{-1}

copolymers and copolymers of MMA with cyclohexyl methacrylate, phenyl methacrylate and t-butyl methacrylate have also been previously examined[47,51]. The latter miscibility maps are described by an ellipse; whereas in the current case when GMA is the comonomer, the miscibility map is hyperbolic in form. The interaction energies for the latter blend systems have been reported elsewhere[47].

BLENDS OF GMA/S WITH TMPC

Blends of tetramethyl polycarbonate (TMPC) and polystyrene are miscible and show *LCST* behaviour[24]. The effect of incorporating GMA as a comonomer into the sytrene polymer on the phase behaviour of these blends was examined. Blend films of TMPC and GMA/S copolymers prepared by hot casting from THF were transparent when the copolymer contained 37.1 wt% or less of GMA. Blends with copolymers containing 43.5 wt% or more of GMA led to films that were cloudy. *Figure 8* shows the T_g behaviour for 50/50 wt% blends as the GMA content of the GMA/S copolymer is varied. Two T_g values were observed for copolymers containing 43.5 wt% GMA or more. *Figure 9* shows the T_g dependence on composition for TMPC blends with three selected GMA/S copolymers. Phase separation on heating was observed for blends of TMPC with the GMA/S copolymer containing 1.6 wt% GMA at 267°C for a 50/50 wt% blend. For blends based on all other copolymers in the miscible region, phase separation was not observed prior to thermal decomposition.

The Flory–Huggins theory combined with the binary interaction model for a copolymer/homopolymer system is:

$$B = B_{13}\phi'_1 + B_{23}\phi'_2 - B_{12}\phi'_1\phi'_2 \qquad (14)$$

Since there is only one miscibility boundary for blends of TMPC with GMA/S copolymers, two other interaction energies are needed at 160°C, the drying temperature, to compute the interaction energy for GMA/TMPC. Prior analysis of blends of TMPC and polystyrene[24] gives $B_{S/TMPC} = -0.14$ cal cm^{-3} at 160°C (from $\Delta P^*_{S/TMPC} =$

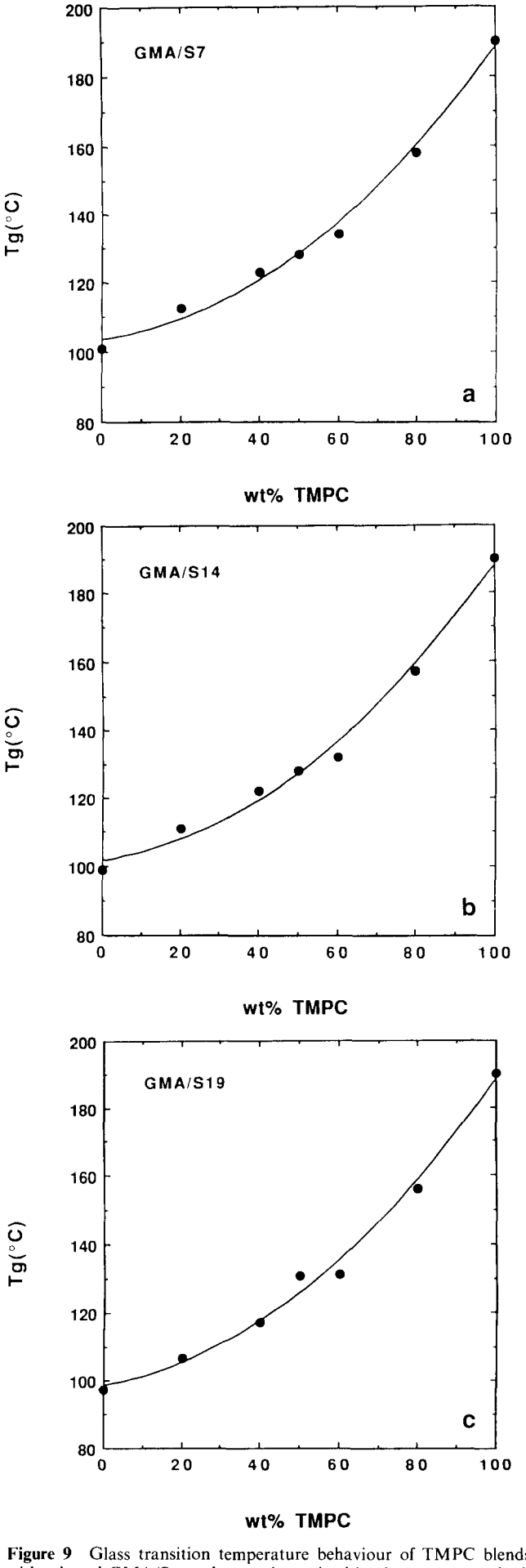

Figure 9 Glass transition temperature behaviour of TMPC blends with selected GMA/S copolymers determined by d.s.c. (onset method) at 20°C min^{-1}

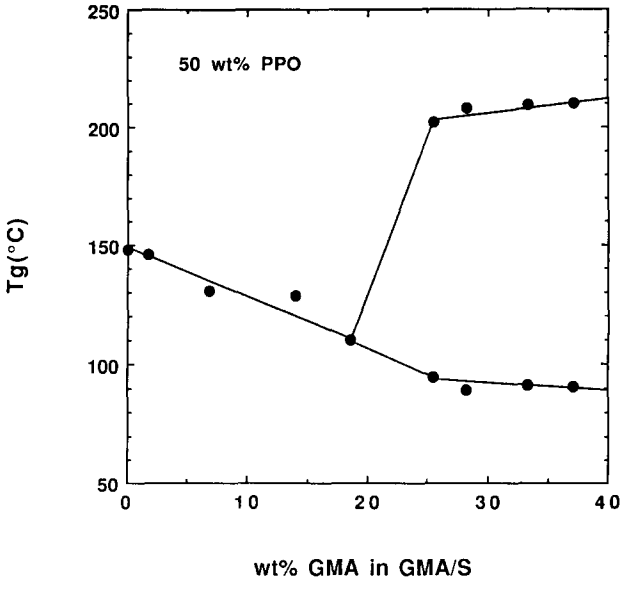

Figure 10 Glass transition temperatures for 50/50 wt% blends of PPO with GMA/S copolymers by d.s.c. (onset method) at 20°C min^{-1}

-0.17 cal cm^{-3}) while the above analysis of blends of GMA/MMA and SAN copolymers leads to $B_{GMA/S} = 1.04$ cal cm^{-3} at 160°C (based on $\Delta P^*_{GMA/S} = 0.99$ cal cm^{-3}). From these values and the miscibility limit, we obtain $0.84 < B_{GMA/TMPC} < 0.97$ cal cm^{-3}. The corresponding $\Delta P^*_{GMA/TMPC}$ ranges from 0.87 to 0.98 cal cm^{-3}. We surmise that $\Delta P^*_{GMA/TMPC}$ is closer to 0.98 cal cm^{-3} since the phase-separation temperature predicted (280°C) using this value is closer to the experimental phase-separation temperature of 267°C for 50/50 blend of TMPC with GMA/S2. In addition, if $\Delta P^*_{GMA/TMPC} = 0.87$ cal cm^{-3}, the calculated bare interaction energy would predict that blends of TMPC with GMA/S43 would be miscible whereas the value $\Delta P^*_{GMA/TMPC} = 0.98$ cal cm^{-3} would indicate that blends of TMPC with GMA/S43 are immiscible, as observed experimentally. Therefore, we can conclude here that $\Delta P^*_{GMA/TMPC}$ is closer to 0.98 cal cm^{-3}, corresponding to $B_{GMA/TMPC} = 0.97$ cal cm^{-3} at 160°C.

BLENDS OF GMA/S WITH PPO

Blends of PPO and polystyrene are miscible at all compositions and do not phase-separate on heating prior to decomposition of the components[22,58–61]. Blends of PPO and GMA/S copolymers containing 18.6 wt% GMA and less, solution cast from chloroform, were found to be transparent and exhibited a single T_g. *Figure 10* shows the T_g behaviour for blends of 50/50 wt% PPO with GMA/S copolymers. *Figure 11* depicts the T_g dependence for PPO blends with selected GMA/S copolymers as the composition of the blend is varied. The miscible blends did not phase-separate prior to decomposition.

Interaction energy densities were calculated using the same method of analysis as performed for blends of TMPC with GMA/S copolymers. In this case, values of $B_{S/PPO}$ and $B_{GMA/S}$ at 180°C (drying temperature of the blends) are used to approximate the interaction energy for the PPO/TMPC pair. Previously[22] we estimated that $\Delta P^*_{S/PPO}$ must be less than -0.42 cal cm^{-3} since blends of PPO/PS do not phase-separate on heating to

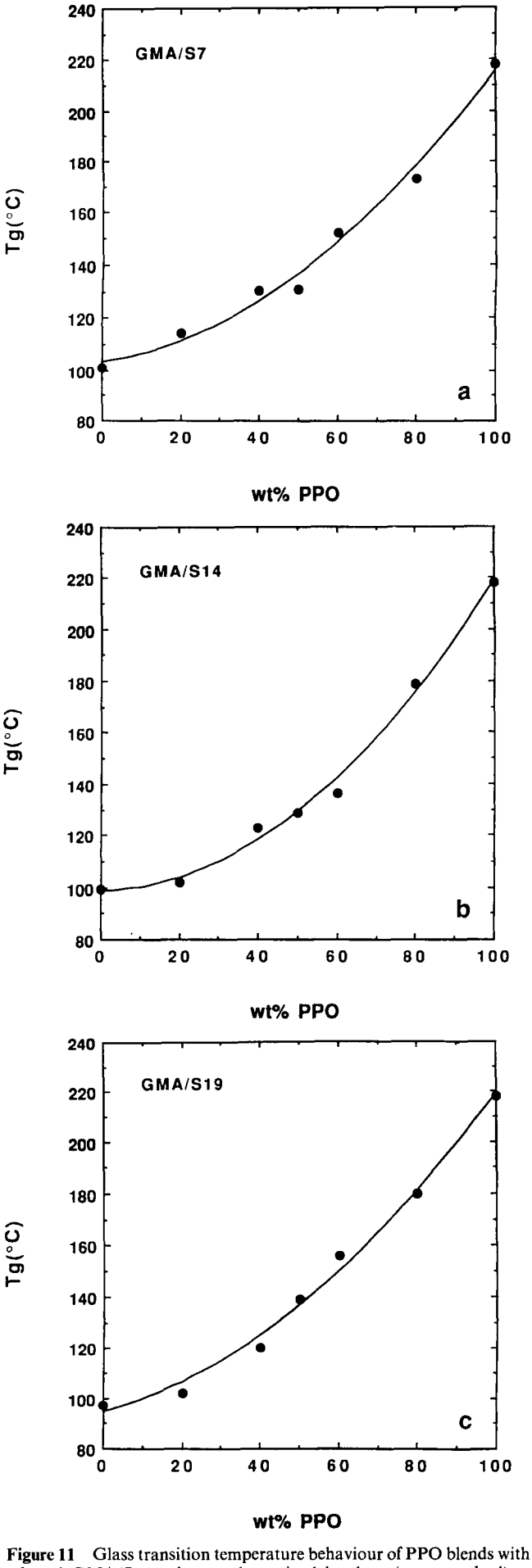

Figure 11 Glass transition temperature behaviour of PPO blends with selected GMA/S copolymers determined by d.s.c. (onset method) at 20°C min^{-1}

Table 7 Comparison of estimated cohesive energy parameters and interaction energies

(a) Homopolymer cohesive energy parameters ((cal cm^{-3})$^{1/2}$)

Polymer	Abbreviations	δ	$(P^*)^{1/2}$
Poly(methyl methacrylate)	PMMA	9.1	11.0
Poly(glycidyl methacrylate)	PGMA	10.0	11.8
Polystyrene	PS	9.5	9.8
Tetramethyl bisphenol A polycarbonate	TMPC	9.5	10.3
Polyacrylonitrile	PAN	13.8	11.4
Poly(2,6-dimethyl-1,4-phenylene oxide)	PPO	9.8	9.9

(b) Interaction energies ((cal/cm^{-3})$^{1/2}$)

Interaction pair	ΔP_{ij}^*	$[(P_i^*)^{1/2}-(P_j^*)^{1/2}]^2$	B_{ij}[a]	T (°C)	$(\delta_i-\delta_j)^2$ by Coleman
S/MMA	0.23	1.51	0.23	100	0.16
S/AN	7.37	2.50	7.07	100	18.5
S/GMA	0.99 to 1.04	4.00	0.92 to 0.98	100	0.25
S/TMPC	−0.17	0.26	−0.14	160	0.00
S/PPO	<-0.42	0.01	<-0.33	180	0.08
GMA/MMA	0.17	0.64	0.15	100	1.00
GMA/AN	2.09 to 2.37	0.16	2.25 to 2.50	100	14.4
GMA/TMPC	0.89 to 0.98	2.25	0.87 to 0.97	160	0.25
GMA/PPO	>3.62	3.61	>3.31	180	0.04
MMA/AN	4.44	0.12	4.42	100	22.1

[a] Note that B_{ij} represent values from the spinodal condition evaluated at the temperatures shown

temperatures of at least 300°C, which translates to $B_{S/PPO} < -0.37$ cal cm^{-3} at 180°C using equation (13). Above we estimated $B_{GMA/S} = 1.04$ cal cm^{-3}. From these two values and the miscibility limit for blends of GMA/S copolymers with PPO, we can estimate two limits: $B_{GMA/PPO} > 2.23$ or $B_{GMA/PPO} > 3.31$ cal cm^{-3}. The corresponding $\Delta P^*_{GMA/PPO}$ is either >2.54 or >3.62 cal cm^{-3}. The limit $\Delta P^*_{GMA/PPO} > 2.54$ cal cm^{-3} indicates that blends of PPO with GMA/S25 would be miscible with a phase-separation temperature above 300°C, whereas $\Delta P^*_{GMA/PPO} > 3.62$ cal cm^{-3} indicates that this blend would be immiscible, as observed experimentally. Therefore, a better representation of the phase behaviour of blends of PPO with GMA/S copolymers is obtained when $\Delta P^*_{GMA/PPO} > 3.62$ cal cm^{-3}. From miscibility limits for blends of PPO with SMMA copolymers[62], we estimate that $B_{MMA/PPO} > 3.2$ cal cm^{-3}, which is of the same order of magnitude as calculated for GMA/PPO. Thus, the estimate for GMA/PPO interaction seems reasonable.

CONCLUSIONS

A broad region of miscibility was obtained for blends of GMA/MMA copolymers with SAN copolymers. Most of the miscible blends did not phase-separate prior to thermal degradation; however, phase-separation temperatures were measured for a few copolymer–copolymer compositions. This system also includes the well known miscibility window for PMMA with SAN copolymers. PGMA was found to be miscible with SAN copolymers containing 32.3 to 58.8 wt% AN and their phase-separation temperatures are all above the degradation limit. Blends of GMA/S copolymers with TMPC and PPO were also examined here, and, in essentially all cases, the miscible blends did not phase-separate prior to thermal degradation.

Interaction energy densities for the various monomer unit pairs were estimated using the binary interaction energy model combined with the Flory–Huggins theory for mapping the copolymer composition regions that show miscibility and with the Sanchez–Lacombe theory for analysis of phase-separation temperatures. These analyses were aided by use of previously determined interaction energies. The binary interaction energies estimated by the two approaches for GMA/MMA and SAN copolymers agree well with other (see *Table 5*). The interaction energies involving GMA as one component were verified, within certain limits, by independent experiments based on the critical molecular-weight approach. The limited extent of observable *LCST* behaviour for blends of TMPC and PPO with GMA/S copolymers resulted in only upper or lower bounds on the interaction energies for these systems. These estimates are listed in *Table 7*. The interaction of GMA with other monomer units is generally more unfavourable than the corresponding interaction with MMA except in the case of acrylonitrile units.

Table 7 lists the solubility parameter for each polymer of interest here estimated by the group contribution method described by Coleman *et al.*[63] and the square root of the characteristic pressure, P^*, obtained by fitting *PVT* data to the Sanchez–Lacombe equation of state. The following equations give estimates of the respective interaction energy densities:

$$B_{ij} = (\delta_i - \delta_j)^2 \tag{15}$$

or

$$\Delta P_{ij}^* = [(P_i^*)^{1/2} - (P_j^*)^{1/2}]^2 \tag{16}$$

when the absolute interaction energy between unlike i and j units is simply the geometric mean of the absolute interaction energy for the two like pairs i–i and j–j. These estimates of the interaction energy densities do not match those deduced from the phase behaviour using either the *LCST* behaviour or the miscibility boundary approach. The experimental interaction energy densities obtained here, on the other hand, will be of value in the design of multicomponent polymer systems involving GMA monomer units for the purpose of reactive processing. Of course, the interaction energies obtained only have utility for predicting phase behaviour when employed within the same theoretical framework from which they were deduced. That is, ΔP^* values have absolute meaning only in the context of the Sanchez–Lacombe theory and B in the Flory–Huggins theory. However, within the limits of the assumptions made, B can be computed from ΔP^* and vice versa via equation (13).

ACKNOWLEDGEMENT

Financial support of this work has been provided by the National Science Foundation Grant, Numbers DMR-89-00704 and DMR-92-15926, administered by the Division of Material Research—Polymers Program.

REFERENCES

1 Fayt, R., Jerome, R. and Teyssie, P. *J. Polym. Sci., Polym. Lett. Edn.* 1981, **19**, 79
2 Fayt, R., Jerome, R. and Teyssie, P. *J. Polym. Sci., Polym. Phys. Edn.* 1981, **19**, 1269
3 Fayt, R., Jerome, R. and Teyssie, P. *J. Polym. Sci., Polym. Phys. Edn.* 1982, **20**, 2209
4 Fayt, R., Hadjiandreou, P. and Teyssie, P. *J. Polym. Sci., Polym. Chem. Edn.* 1985, **23**, 337
5 Fayt, R., Jerome, R. and Teyssie, P. *Makromol. Chem.* 1986, **187**, 837
6 Fayt, R., Jerome, R. and Teyssie, P. *J. Polym. Sci., Polym. Lett. Edn.* 1986, **24**, 25
7 Ouhadi, T., Fayt, R., Jerome, R. and Teyssie, P. *J. Polym. Sci., Polym. Phys. Edn.* 1986, **24**, 973
8 Triacca, V., Ziaee, S., Barlow, J. W., Keskkula, H. and Paul, D. R. *Polymer* 1991, **32**, 1401
9 Lu, M., Keskkula, H. and Paul, D. R. *Polym. Eng. Sci.* 1994, **34**, 33
10 Lu, M., Keskkula, H. and Paul, D. R. *Polymer* 1993, **34**, 1874
11 Shaver, G. P., M.S. Thesis, University of Texas at Austin, 1989
12 Stewart, M. E., George, S. E. and Miller, R. L. *Polym. Eng. Sci.* 1993, **33**, 675
13 Sanchez, I. C. and Lacombe, R. H. *J. Phys. Chem.* 1976, **80**, 2352
14 Sanchez, I. C. and Lacombe, R. H. *J. Polym. Sci., Polym. Lett. Edn.* 1977, **15**, 71
15 Sanchez, I. C. and Lacombe, R. H. *Macromolecules* 1978, **11**, 1145
16 Sanchez, I. C. *Polymer* 1989, **30**, 471
17 Callaghan, T. A., Ph.D. Dissertation, University of Texas at Austin, 1992
18 Callaghan, T. A. and Paul, D. R. *J. Polym. Sci., Polym. Phys. Edn* in press
19 Callaghan, T. A. and Paul, D. R. *Macromolecules* 1993, **26**, 2439
20 Callaghan, T. A., Takakuwa, K., Paul, D. R. and Padwa, A. R. *Polymer* 1993, **34**, 3796
21 Callaghan, T. A. and Paul, D. R. *J. Polym. Sci., Polym. Phys. Edn.* in press
22 Gan, P. P., Paul, D. R. and Padwa, A. R. *Polymer* in press
23 Kim, C. K. and Paul, D. R. *Polymer* 1992, **33**, 2089
24 Kim, C. K. and Paul, D. R. *Polymer* 1992, **33**, 1630
25 Kim, C. K., Ph.D. Dissertation, University of Texas at Austin, 1992
26 Dobinson, B. Hofmann, W. and Stark, B. P. 'The Determination of Epoxide Groups', Pergamon, London, 1969
27 Jungnickel, J. L., Peters, E. D., Polgar, A. and Weiss, F. T. 'Organic Analysis', Interscience, New York, 1953
28 Siggia, S. 'Quantitative Organic Analysis via Functional Groups', Wiley, New York, 1963
29 Nishimoto, M., Keskkula, H. and Paul, D. R. *Polymer* 1989, **30**, 1279
30 McMaster, L. P. *Adv. Chem. Ser.* 1975, **142**, 43
31 Naito, K., Johnson, G. E., Allara, K. L. and Kwei, T. K. *Macromolecules* 1978, **11**, 1260
32 Cowie, M. G. and Lath, D. *Makromol. Chem., Macromol. Symp.* 1988, **16**, 103
33 Chiou, J. S., Paul, D. R. and Barlow, J. W. *Polymer* 1982, **23**, 1543
34 Kressler, J., Kammer, H. W. and Klostermann, K. *Polym. Bull.* 1986, **15**, 113
35 Stein, D. J., Jung, R. H., Illers, K. H. and Hendus, H. *Angew. Makromol. Chem.* 1974, **36**, 89
36 Bernstein, R. E., Cruz, C. A. and Paul, D. R. *Macromolecules* 1977, **10**, 681
37 Fowler, M. E., Barlow, J. W. and Paul, D. R. *Polymer* 1986, **28**, 1177
38 Paul, D. R. and Newman, S. 'Polymer Blends', Academic Press, New York, 1987
39 Boyer, R. F. *Macromolecules* 1982, **15**, 774
40 Quach, A. and Simha, R. *J. Appl. Phys.* 1971, **42**, 4592
41 Zoller, P. *J. Polym. Sci., Polym. Phys. Edn.* 1978, **16**, 1261
42 Cowie, J. M. G., Elexpuru, E. M. and McEwen, I. J. *Polymer* 1992, **33**, 1993
43 Cowie, J. M. G. *Makromol. Chem., Macromol. Symp.* 1992, **58**, 63
44 Cowie, J. M. G. and Elexpuru, E. M. *Eur. Polym. J.* 1992, **28**, 623
45 Cowie, J. M. G., Elexpuru, E. M. and McEwen, I. J. *J. Polym. Sci., Polym. Phys. Edn.* 1991, **29**, 407
46 Cowie, J. M. G., Reid, V. M. C. and McEwen, I. J. *Polymer* 1990, **31**, 905
47 Gan, P. P., Ph.D. Dissertation, University of Texas at Austin, 1994
48 Fukuda, T. and Inagaki, H. *Pure Appl. Chem.* 1983, **55**, 1541
49 Fukuda, T., Nagata, M. and Inagaki, H. *Macromolecules* 1984, **17**, 548
50 Fukuda, T., Nagata, M. and Inagaki, H. *Macromolecules* 1986, **19**, 1411
51 Nishimoto, M., Keskkula, H. and Paul, D. R. *Macromolecules* 1990, **23**, 3633
52 Brannock, G. R., Ph.D. Dissertation, University of Texas at Austin, 1990
53 Brannock, G. R., Barlow, J. W. and Paul, D. R. *J. Polym. Sci., Polym. Phys. Edn.* 1990, **28**, 871
54 Brannock, G. R., Barlow, J. W. and Paul, D. R. *Macromolecules* 1991, **29**, 413
55 Kim, C. K. and Paul, D. R. *Polymer* 1992, **33**, 4941
56 Russell, T. P., Hjelm, R. P. and Seeger, P. A. *Macromolecules* 1990, **23**, 890
57 Russell, T. P. *Macromolecules* 1993, **26**, 5819
58 Schultz, A. R. and Gendron, B. M. *J. Appl. Polym. Sci.* 1972, **16**, 461
59 Stoelting, J., Karasz, F. E. and MacKnight, W. J. *Polym. Eng. Sci.* 1970, **10**, 133
60 Tucker, P. S. and Paul, D. R. *Macromolecules* 1988, **21**, 2801
61 Kambour, R. P., Bendler, J. T. and Bopp, R. C. *Macromolecules* 1983, **16**, 753
62 Kressler, J., Krammer, H., Morgenstern, U., Litauski, B., Berger, W. and Karasz, F. E. *Makromol. Chem.* 1990, **191**, 243
63 Coleman, M. M., Graf, J. F. and Painter, P. C. 'Specific Interactions and the Miscibility of Polymer Blends', Technomic, Lancaster, PA, 1991